Rev. Mexicana Astron. Astrof., 9, 119-125 (1984)

THE STRUCTURE AND DYNAMICS OF THE Car II ("KEYHOLE") REGION IN THE CARINA NEBULA

J.A. López and J. Meaburn

Department of Astronomy, University of Manchester

Received 1984 April 30

RESUMEN

Se han obtenido espectros de dispersión baja e intermedia de la nebulosa Car II ("El ojo de la cerradura"), la cual se encuentra localizada al norte de η Carinae en NGC 3372 (= RCW 53), con el fin de investigar el origen de las componentes de alta velocidad sobrepuestas sobre las alas extendidas de las líneas de Hα y Hβ, reportadas por Elliott (1979) , y su posible asociación con un remanente de supernova. No se han encontrado evidencias de dicho remanente en nuestros espectros, los cuales muestran ser característicos de regiones H II de excitación moderada. Sin embargo, se confirman las componentes de alta velocidad en las líneas de Balmer. Se encuentra que estas componentes se extienden sobre un intervalo de velocidades de $\sim$ 1150 km s^{-1} con respecto a la componente central principal. Se ha detectado un continuo azul notable en aquellos espectros más cercanos a η Carinae y la estrella O3 HDE 303308, donde se confirma que el mecanismo responsable de este efecto es la dispersión de luz estelar. Se ha encontrado que la estratificación de material en diferentes grados de excitación está presente en la región. Se discuten varios modelos que pudieran explicar las estructuras de alta velocidad en las líneas de Balmer en Car II y su vecindad.

ABSTRACT

A set of intermediate and low dispersion spectra have been obtained of the Car II ("Keyhole") nebula, located to the north of η Carinae in NGC 3372 (= RCW 53), in order to search for clues on the origin of the high velocity components superimposed on the extended wings of the Hα and Hβ lines reported by Elliott (1979) and their possible association with a supernova remnant. No apparent evidence of such a SNR is found in our spectra which closely resemble those of classical H II regions of moderate excitation. Although, the high velocity components in the Balmer lines are confirmed; it has been found that these components extend over a velocity range of $\sim$ 1150 km s^{-1}. A distinct blue continuum is detected in those spectra closer to η Carinae and the O3 star HDE 303308, where light scattering is confirmed as the mechanism responsible for this effect. Stratification of material in different degrees of excitation is present over the whole region. Several models that might explain the high velocity structure of the Balmer lines in Car II and its vicinity are discussed.

Key words: **H II REGIONS – SUPERNOVA REMNANT**

I. INTRODUCTION

The Carina nebula is a complex aggregate of ionized and neutral gas and dust and contains the most massive stars in the galaxy. Located at a distance of 2.7 kpc, it covers an area of approximately 4 square degrees. The kinematics of the nebula are very complicated. Two different types of dynamics appear to be involved. On one hand, the multitude of massive OB-type and WR stars in the region form localized expanding "bubbles" when their energetic winds interact with the rich surrounding interstellar medium. In this context, multiple velocity components in the blue H and K Ca II lines and in the *UV* range have been detected in the past covering a velocity range from $\sim$ 200 to 550 km s^{-1}, respectively (cf. Walborn and Hesser 1982; Laurent, Paul, and Pettini 1982). These motions imply violent interactions of the stellar winds from these massive stars with the ambient material. On the other hand, and superimposed on this comparatively small scale disturbance of the nebula, radio observations of H_2CO (Gardner, Dickel, and Whiteoak 1973), OH (Dickel and Wall 1974), CO (de Graw *et al.* 1981); H109α and H158α recombination lines (Gardner *et al.* 1970; Hutchmeir and Day 1975) and optical Hα and [O III] Fabry-Pérot observations covering large areas of the nebula (Deharveng and Maucherat 1975; Meaburn, López and Keir 1984, respectively) show extensive line splitting over the whole face of the nebula. The typical splitting of the profiles is $\sim$ 40 km s^{-1}. These studies reveal systematic trends in the motions of the gas associated with the nebula on a much larger scale, differing essentially in its dynamics from the localized "bubbles" embedded in this giant H II region. The most extensive optical coverage of the nebula is the study of Meaburn, López and Keir (1984)

where these superimposed types of motion are discussed.

In the northern region of the Carina nebula there are two sources of strong thermal radio emission. They are known as Car I and Car II. These sources are located in the neighborhood of the open clusters Trumpler 14 and 16, respectively. The object η Carinae belongs to the Trumpler 16 cluster, and to the north of η Carinae there is a distinct filamentary nebulosity in whose center is located the Car II source. This region is known as the "keyhole" as a consequence of its morphology (see Figures 1 and 2, Plates 1 and 2). It was on this area that Elliott (1979) discovered that the line profiles of the Hα and Hβ lines have wings with FWHM of $\sim$ 650 km s^{-1}. These wings are absent in the profiles of the [N II] $\lambda\lambda$6548,84, [O III] $\lambda\lambda$4959,5007 and [S II] $\lambda\lambda$6717, 6731 lines from the same region. These very high velocity components together with a possible association with an X-ray and a non-thermal radio continuum source led Elliott to suggest that the filamentary shell was a supernova remnant. Recently this interpretation has been challenged by Retallack (1983) who, from high angular resolution aperture-synthesis radio continuum observations at 1415 MHz, finds that the radio structure of the region matches closely the optical emission with no evidence of a non-thermal component. The non-thermal component quoted by Elliott refers to the one detected by Jones (1973) lying $\sim$ 14 arcmin away. In addition, the X-ray emission can be accounted for by the hot gas produced by the numerous massive stars in the area (cf. Seward *et al.* 1979).

The aim of the present work was to investigate the full extent of the region emitting Hα with broad wings and to relate this to deep photographs of the filamentary shell. For this purpose both low and intermediate dispersion spectra and new Schmidt photographs have been obtained.

II. OBSERVATIONS

a) *Spectra*

The observations were made with the image tube grating spectrograph mounted at the Cassegrain focus of the 1.9-m. SAAO telescope. The detector was the reticon photon counting system (RPCS). This is a solid state device which achieves photon counting in two parallel one-dimensional arrays each containing 1872 pixels. Each of these arrays record simultaneously photon-events from two adjacent positions separated by 30 arcsec on the sky (channels 1 and 2). A low dispersion grating was used to examine the spectral range $\sim$ 3500-6900 Å with a reciprocal dispersion of 210 Å mm^{-1}. An aperture slit 3.6 arcsec wide and 6.0 arcsec long was used. For higher spectral resolution a different grating which gave 50 Å mm^{-1} was used to cover the [N II]-Hα-[S II] and Hβ-[O III] ranges. The aperture slit was in these cases 1.8 X 6.0 arcsec. All the spectra were divided by the spectrum of a white light source (flat-field) to correct for pixel to pixel variations of the detector and calibrated in wavelength using separate exposures of a Cu-Ar arc. For the calibration of the low dispersion spectra in units of erg cm^2 s^{-1} Å^{-1}, a sky signal obtained off the Carina nebula was subtracted and the effects of atmospheric and interstellar extinction corrected for. In the latter case, the correction curve of Seaton (1979) with a logarithmic extinction coefficient $c \cong 0.32$, obtained from the Hα/Hβ ratios, was used. The standard star EG99 (Oke 1974) was used for the absolute calibration.

Since two different positions were recorded simultaneously in every observation, they have been labeled with letters for every pair of observations and numbers denoting the corresponding channel. The positions that were observed are listed in Table 1 and shown in Figure 3 against a sketch of the nebula. Positions A1 and A2 are located near the center of the shell structure and the sequence proceeds counterclockwise. The position of the infrared source (Harvey, Hoffman, and Campbell 1979) and the thermal radio source (Retallack 1983) are also indicated in this diagram. Also in Table 1 is shown whether low (LDS) or intermediate (IDS) dispersion spectra, or both were obtained for that particular position.

Figures 4*a* and 4*b* show the observed IDS Hα profiles. The separate high velocity components which are superimposed on the broad wings and that consistently appear in many of the profiles are arrowed. The mean absolute wavelengths and heliocentric radial velocities of the main separate components in the Hα profiles are given in Table 2. Similarly, components in the Hβ profile from positon C2 are also listed in this table.

TABLE 1

POSITIONS OF THE OBSERVED INTERMEDIATE AND LOW DISPERSION SPECTRA[a]

Position	(1950)		IDS	LDS
A1	$10^h\,42^m\,55^s$	$-59°\,23'\,12''$	*	*
B1	42 49	22 58	*	
C1	42 46	23 32	*	
D1	42 39	22 31	*	*
E1	42 45	22 40	*	
F1	42 52	22 30	*	*
G1	43 00	22 50	*	*
H1	43 00	23 17	*	
I1	42 59	24 03		*

a. The positions of the channels 2 are displaced westward by 30 arcsec from those of the corresponding channel 1, and have the same type of intermediate or low dispersion spectra.

b) *Schmidt Photographs*

The enlargements in Figs. 1 and 2 (Plates 1 and 2) are from photographs taken with the 1.2-m UK Schmidt telescope through two interference filters (Meaburn 1978) centered on [S II] and Hα plus [N II], respectively,

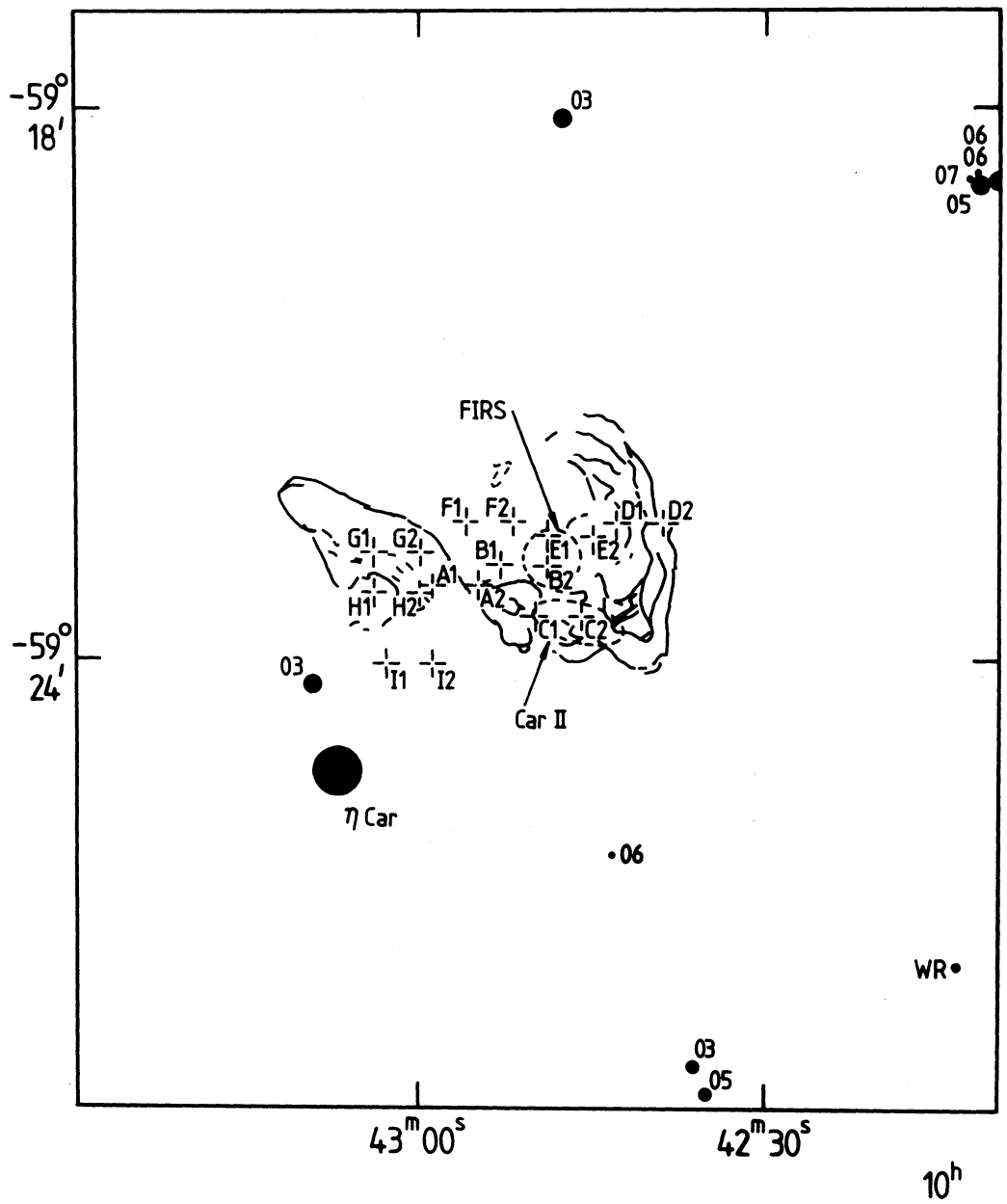

ig. 3. The positions of the observed low and high dispersion spectra are marked against this sketch of the filamentary nebula that covers ıe same area as that of Figs. 1 and 2, Plates 1 and 2). Some of the most massive stars in the region have been indicated. Another three)3 stars that belong to the Tr 14 cluster lie just outside the area shown, slightly further northwest of the cluster in the upper right side f the sketch. The positions of the far infrared source, FIR (Harvey *et al.* 1979) and the peak of the Car II thermal radio source (Retallack 983) are enclosed whithin dashed lines.

III. RESULTS

a) *Photographs and Low Dispersion Spectra*

Distinct morphological differences are apparent ıetween the photographs in Plates 1 and 2. The fila- ıentary shell structure is best revealed in the light of he [S II] lines in Plate 1, whereas the prominence of the lark lanes and the complexity of the nebular region is evident in the Hα print in Plate 2. Considering also the photographs presented by Deharveng and Maucherat (1975) in the light of [N II], Hβ and [O III], it becomes clear that a strong stratification of different degrees of excitation, occurs. The highly ionized species (e.g., [O III]) occupy distinctly separate regions from those of low ionization potential ([N II], [S III]).

The Hβ/[O III] and [O II]/[O III] ratios observed in the LDS reveal a region of moderate excitation with

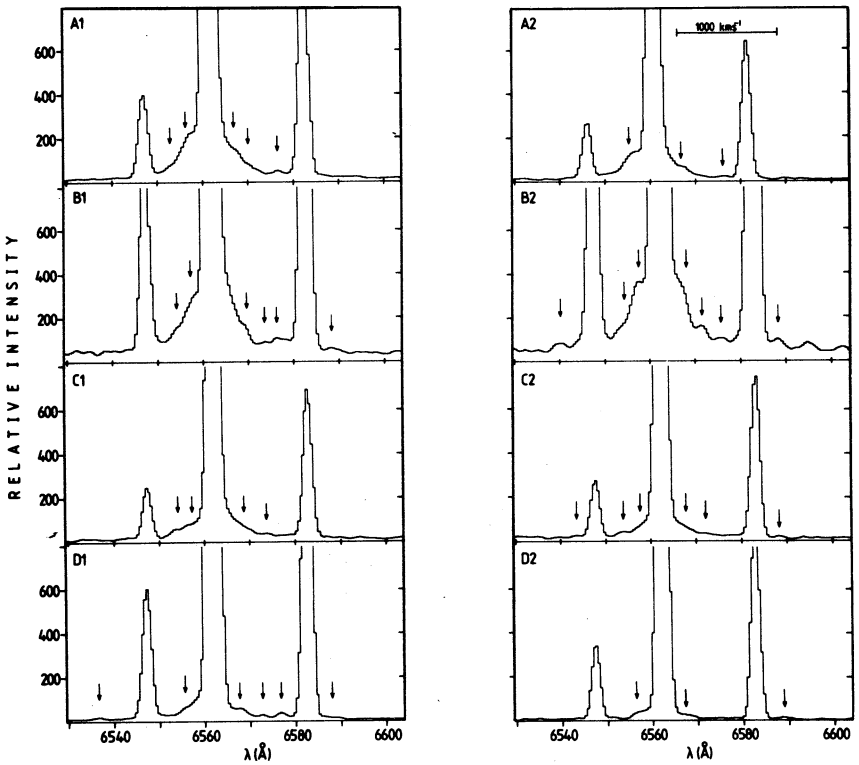

Fig. 4*a*. The intermediate dispersion spectra of Hα observed over the face of the filamentary nebulosity. Those high velocity components that are conspicuous and consistently present in most of the observed positions are arrowed. Note that the [N II] lines do not show wings at all. The spectra have been multiplied by constant factors to normalize them with respect to the exposure with longest dwell time. The relative intensities are, therefore, in the same scale to an accuracy of ± 10%.

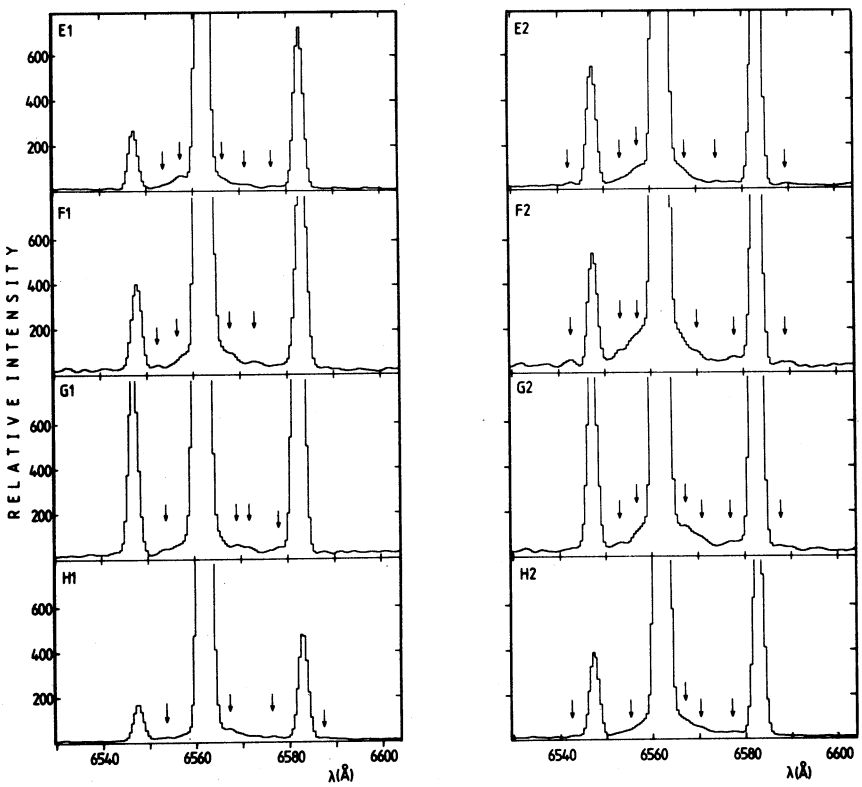

Fig. 4*b*. As for Figure 4*a*.

TABLE 2

MEAN ABSOLUTE WAVELENGHTS AND RADIAL VELOCITIES OF THE MAIN HIGH VELOCITY COMPONENTS IN Hα AND Hβ

Wavelength (A)	$V_{hel.}$ (km s^{-1})
Hα	
6542	−956
6554	−408
6557	−271
6569	278
6576	598
6588	1146
Hβ[a]	
4848	−826
4852	−576
4869	470
4876	870
4880	1148

a. From position C2.

fairly smooth variations across the sampled area. Exceptions are: Position A1 and A2 which show a distinct difference in the ratio of [O II] to [O III], indicating that A2 is of lower excitation than A1. Positions I1 and I2 and D1 and D2, show the brightest oxygen lines; the former has the weakest [S II] lines whereas the latter has the brightest of the sample. All this coincides with what one would expect from the interference filter photographs. The continuum of atomic recombination origin shows in most of the spectra substantial contribution of starlight scattered by the embedded dust. This is particulary the case in positions I1 and I2, where a distinct blue continuum rising towards shorter wavelengths is observed. This is illustrated in Figure 5, where the spectra of positions D2 and I2 are displayed, amplified and at full scale in order to facilitate comparison. The positions I1 and I2 are the nearest to η Carinae and the O3 star HDE 303308, therefore scattered light most likely originates from these sources. These positions coincide with a blue patch of nebulosity that is particularly well revealed in the blue photograph of the area

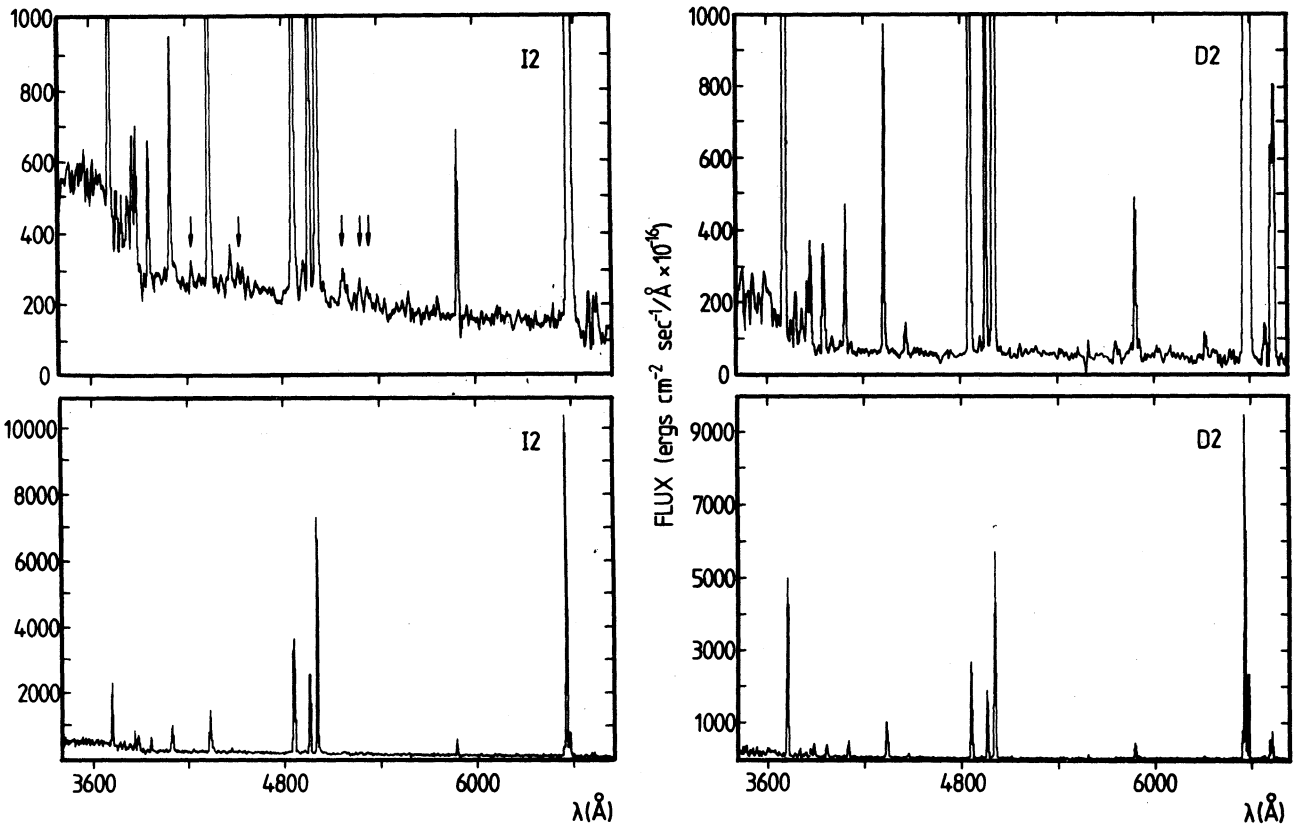

Fig. 5. The atomic recombination continuum in the low dispersion spectra shows substantial contribution of starlight scattered in the embedded dust. This is particularly the case for positions I1 and I2 that show scattered light from η Carinae and, most probably from the O3 star HDE 303308 as well. Positions D2 (from the arc-edge of the nebula) and I2 are shown amplified (above) and at full scale (below) in order to facilitate comparison. Arrows in the amplified spectrum of position I2 point to Fe II emission features reflected from η Carinae.

presented by Gardner *et al.* (1970). Moreover, reflected light from η Carinae has been reported by Walborn and Liller (1975) within this blue patch. The spectra of positions I in fact shows Fe II emission features (indicated in Figure 5) similar to those encountered in the spectrum of η Carinae implying that cloud "D" Walborn and Liller (1977) and positions I1 and I2 in this work are coincident.

None of the LDS reveals emission lines which could relate the filamentary shell to a SNR. Only the Balmer and Pickering series of H and He I, respectively, and forbidden lines of [O III], [O II], [N II] and [S II] are apparent in the spectra. Furthermore, the observed line ratios of Hα/[N II] and Hα/[S II] from the bright filament (corrected for the surrounding H II region) were marked on the diagnostic diagrams of Sabbadin, Minello, and Bianchini (1977). From this comparison, radiative rather than collisional ionization is indicated for this filamentary nebulosity. This seems to rule out a supernova origin. Apart from this observational evidence, a further argument against the presence of a SNR in Car II is that evolutionary time scales for SNR progenitors are $> \sim 3 \times 10^6$ yr. while the age of the OB association is only $\sim 10^6$ yr. (Turner *et al.* 1980). Laurent *et al.* (1982) have also discussed the possibility of a SNR in the region in order to account for anomalous chemical abundances observed in blue shifted components of their *UV* interstellar lines. They argue that either a very young Supernova explosion has occurred $\sim 2 \times 10^3$ yr. ago inside a "hot, rarified cavity" and the SNR is then expanding freely until it encounters the expanding shell, in which case it is difficult to observe it at this stage or, that the SNR originated from a runaway star which escaped a nearby older cluster. In view of the lack of any trace of non-thermal emission in Car II or the immediate neighborhood (Retallack 1983) these possibilities seem somewhat improbable. The present arguments and observations strongly suggest that the bright [S II] filamentary shell that surrounds Car II is composed of radiatively ionized fronts at the boundaries of dense clouds rather than a shock excited region. Harvey *et al.* (1979) have arrived at a similar conclusion from their far infrared observations. They find that their data are compatible with thermal radiation from heated dust in the dark cloud as opposed to a compact hot central source.

b) *The Intermediate Dispersion Spectra*

The IDS shown in Figures 2*a* and *b*, confirm the observations of Elliott (1979) of very high velocity structure in the wings of Hα. In the present work, these high velocities have been found to exist over a much wider range in velocity (> 1000 km s^{-1}) than previously reported and, over the whole optical face of the filamentary shell. No wing structure at all is seen in the forbidden lines. It is worth noting that the high velocity components are always nearly symmetrical about the main narrow component (see Figures 4*a* and 4*b*). However, no clear pattern is detected from these high velocity motions over the filamentary shell. For instance, there are no clear velocity gradients in the spatial distribution of the high velocity components. Whether or not these high velocity flows are somehow related to the low velocity expansion of the Carina nebula, which was suggested to be occurring by Dickel (1974), Hutchmeier and Day (1975) and Deharveng and Maucherat (1975) from the splitting of radio and optical emission over the Car II region; and/or to the verly large scale motions discovered by Meaburn, López and Keir (1984) over the entire extent of the Carina Nebula, is not clear at the moment. The only, very limited, indication of a gradient in velocity in the outer regions of the filamentary shell is provided by position D2 (see Figures 3 and 4*a*). This is located in the west arc-edge of the nebula and the profile of this region shows a diminished structure in the wings of the Hα profile.

IV. DISCUSSION

a) *Energy Considerations*

The Car II region has enough massive stars producing winds and ionizing photons in its neighborhood (see Figure 1) to account for the energetic phenomena of this region, like the high velocity gas, the difusse X-ray emission and the thermal radio and far infrared sources. For instance, the mechanical power, L_W, available from the winds of only the O3, WR stars and η Carinae is approximately $2 - 4 \times 10^{38}$ erg s^{-1} (depending on whether η Carinae is counted as a WR-type star or an outstanding object with $dM/dt \sim 10^{-3}$ $M_\odot$ yr^{-1} and $v_\infty = 600$ km s^{-1}, respectively). The Car II thermal radio-source requires a Lyman continuum flux, L_c, of 5.5×10^{49} photons s^{-1} (Retallack 1983), a requirement easily provided by HDE 303308 or, approximately two O6-type stars. Similarly, the total integrated far-infrared-luminosity of Car II is $L_{FIR} \sim 2 \times 10^4$ $L_\odot$, whereas the luminosity available to power this emission is of the order of 3×10^5 $L_\odot$ (Harvey *et al.* 1979). In the same way, it can be seen that the stellar winds of the massive stars are capable of accounting for the integrated X-ray luminosity of Carina (Seward and Chlebowski 1982). Therefore, it is concluded that there is apparently no need to invoke a supernova-type event to explain the energetic phenomena in this region.

b) *Models*

Several possible origins for the high velocity components in the Hα and Hβ lines from this nebular region are now considered. According to the arguments and observational evidence presented in previous sections, it will be assumed that the high velocity components do not originate from a supernova remnant. Other possibilities could be:

1) *Electron scattering*. The winds from the early-type stars in Carina must interact with the surrounding mate-

rial to produce coronal temperatures that are revealed well in the X-ray maps of Seward and Chlebowsky (1982). The high temperatures and densities that become involved in these processes are adequate conditions to produce significant contributions to the wings of the Balmer line profiles from electron scattering (see for example López and Meaburn 1983 and references therein). Although this is a plausible mechanism to explain the extended wings observed *only* in the Hα and Hβ lines in this region, it cannot account for the distinct separate components (arrowed in Figures 4*a* and 4*b*) which are apparent on most of the observed positions superimposed on the wings.

2) *Obscured internal source(s)*. Massive OB-type and WR stars have mass loss rates of $\sim 10^{-6}$ to 10^{-5} $M_\odot$ yr^{-1}, and terminal velocities in the range of 1000-4000 km s^{-1}. If these winds can be collimated by some means, like density gradients in the ambient material, then little energy is lost over the distance that the flows are confined. A similar picture has been discussed by Barral *et al*. (1982) in the case of the "poly-polar" nebula NGC 6302. However, there is no evidence of the presence of internal sources of such winds within Car II. The far infrared source detected by Harvey *et al*. (1979) indicates thermal radiation from heated dust in the dark cloud; no compact sources are reported in the region. It is worth pointing out in passing, that the positions of the far infrared and the thermal radio sources are not spatially coincident (see Figure 3).

3) *Winds from external sources*. A third possibility that would be worth exploring theoretically (outside the scope of the present paper) is whether or not the high velocity motions could be the consequence of collimated flows, driven by the winds from the very massive stars which are well displaced from the filamentary nebulosity (see Figure 3). These flows could be channeled along passages between denser neutral clouds towards the filamentary nebulosity, where they might interact to give the broad wings that are observed. If the flows from these energetic winds collide in the Car II region, one might expect here an enhancement of diffusse X-ray emission, something that is not clearly seen for this particular region from the maps of Seward and Chlebowsky (1982), although extensive diffuse X-ray emission is observed in the near vicinity. Absorption by foreground cool gas may be obscuring the X-ray emission from Car II.

V. CONCLUSIONS

It has been found that high velocity separate components superimposed on extended wings are present in the Hα line over the entire extent of the filamentary nebulosity in the vicinity of the Car II thermal radio-source, covering a range in velocities of over 1000 km s^{-1} with respect to the central main component. These motions are not detected in other spectral emission-lines nor in *UV*, optical or radio observations of previous investigations. The presence of a supernova remnant as the cause of these motions has been discarded on the basis of the present observational evidence. Alternative explanations on the possible origin of these high velocity components have been put forward. Further high spatial and spectral resolution observations extending the area covered in this work will be necessary to decide on the models discussed above for a better understanding of this important region of massive star formation.

We wish to thank the staff of SAAO for their support during our observing visit in May 1983 and to the SERC for sponsoring it. J.M. is grateful to the S.E.R.C. for his Senior Fellowship and J.A.L. to the Universidad Nacional Autónoma de México for financial support. We also thank the U.K. Schmidt Unit for obtaining the photographs and to Mr. W.V. Garner for printing them so well.

REFERENCIAS

Barral, J.F., Cantó, J., Meaburn, J., and Walsh, J.R. 1982, *M.N.R.A.S.*, **199**, 817.
de Graw, T., Lindholm, S., Fitton, B., Beckman, J., Israel, F.P., Nieuwenhuijzen, H., and Vermue, J. 1981, *Astr. and Ap.*, **102**, 257.
Deharveng, L. and Maucherat, M. 1975, *Astr. and Ap.*, **41**, 27.
Dickel, H.R. 1974, *Astr. and Ap.*, **31**, 11.
Dickel, H.R. and Wall, J.V. 1974, *Astr. and Ap.*, **31**, 5.
Elliott, K.H. 1979, *M.N.R.A.S.*, **186**, 9p.
Gardner, F.F., Milne, D.K., Mezger, P.G., and Wilson, T.L. 1970, *Astr. and Ap.*, 7, 349.
Gardner, F.F., Dickel, H.R., and Whiteoak, J.B. 1973, *Astr. and Ap.*, **23**, 51.
Harvey, P.M., Hoffman, W.F., and Campbell, M.F. 1979, *Ap.J.*, **227**, 114.
Hutchmeier, W.K. and Day, G.A. 1975, *Astr. and Ap.*, **41**, 153.
Jones, B.B. 1973, *Australian J. Phys.*, **26**, 545.
Laurent, C., Paul, J., and Pettini, M. 1982, *Ap. J.*, **260**, 163.
López, J.A. and Meaburn, J. 1983, *M.N.R.A.S.*, **204**, 303.
Meaburn, J. 1978, *Appl. Optics*, **17**, 127.
Meaburn, J., López, J.A., and Keir, D. 1984, *M.N.R.A.S.*, in press.
Oke, J.B. 1974, *Ap. J. Suppl.*, **27**, 21.
Retallack, D.S. 1983, *M.N.R.A.S.*, **204**, 669.
Sabbadin, F., Minello, S., and Bianchini, A. 1977, *Astr. and Ap.*, **60**, 147.
Seaton, M.J. 1979, *M.N.R.A.S.*, **187**, 73p.
Seward, F.D., Forman, W.R., Giacconi, R., Griffiths, R.E., Hamden, F.R., Jr., Jones, C., and Pye, J.P. 1979, *Ap. J.*, **234**, L55.
Seward, F.D. and Chlebowsky, T. 1982, *Ap. J.*, **256**, 530.
Turner, D.G., Grieve, G.R., Herbst, W., and Harris, W.E. 1980, *A.J.*, **85**, 1193.
Walborn, N.R. 1982, *Ap. J. Suppl.*, **48**, 145.
Walborn, N.R. and Liller, M.H. 1977, *Ap. J.*, **211**, 181.
Walborn, N.R. and Hesser, J.E. 1982, *Ap. J.*, **252**, 156.

J. Alberto López and John Meaburn: Department of Astronomy, University of Manchester, Manchester, M13 9 PL, Great Britain.

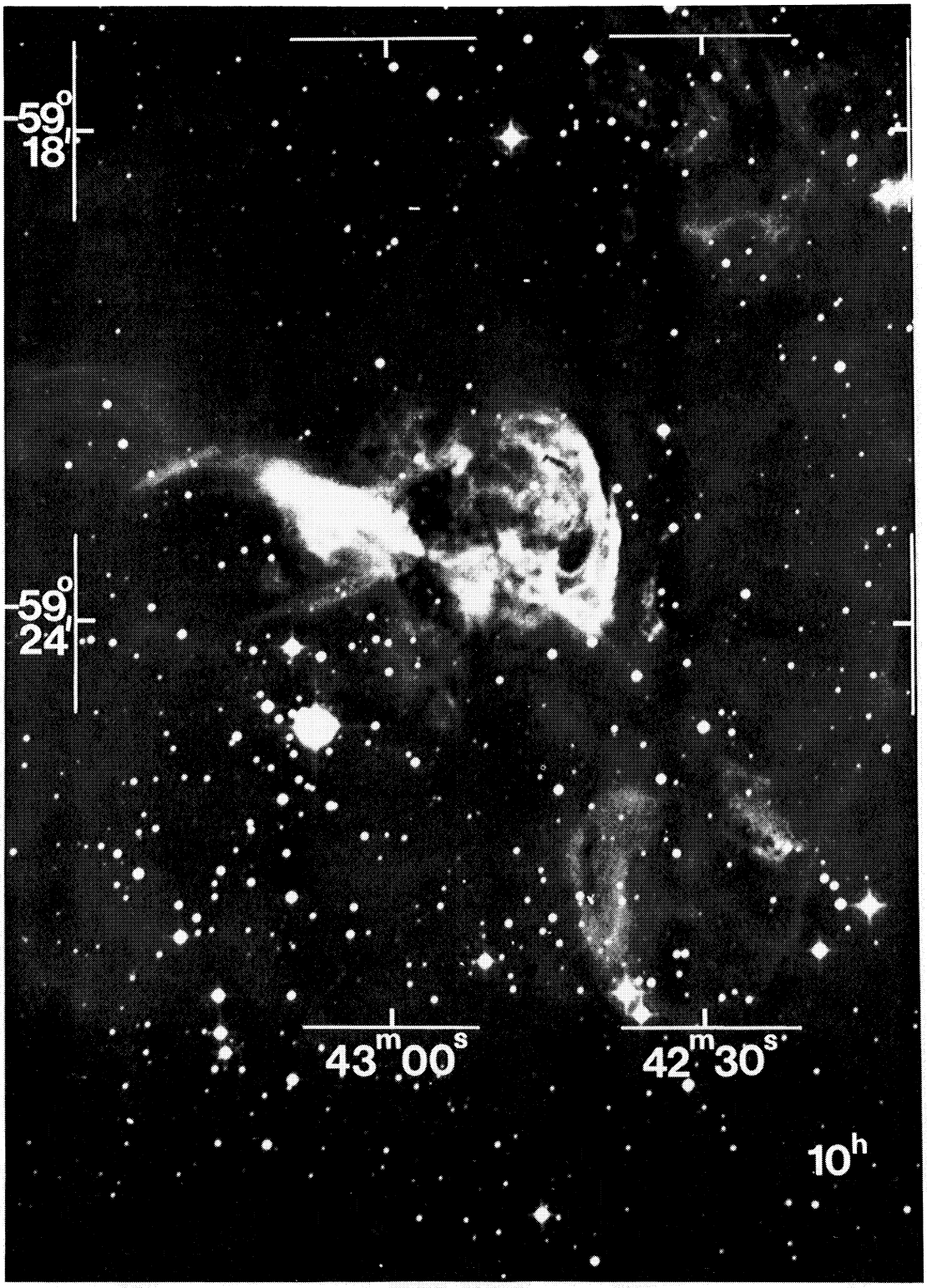

Fig. 1 (Plate 1). An enlargement from a Schmidt plate taken through an interference filter centered on the [S II] λλ6717, 6731 emission lines. The filamentary structure of the nebulosity at the north of η Carinae (the brightest object in the plate) is apparent.

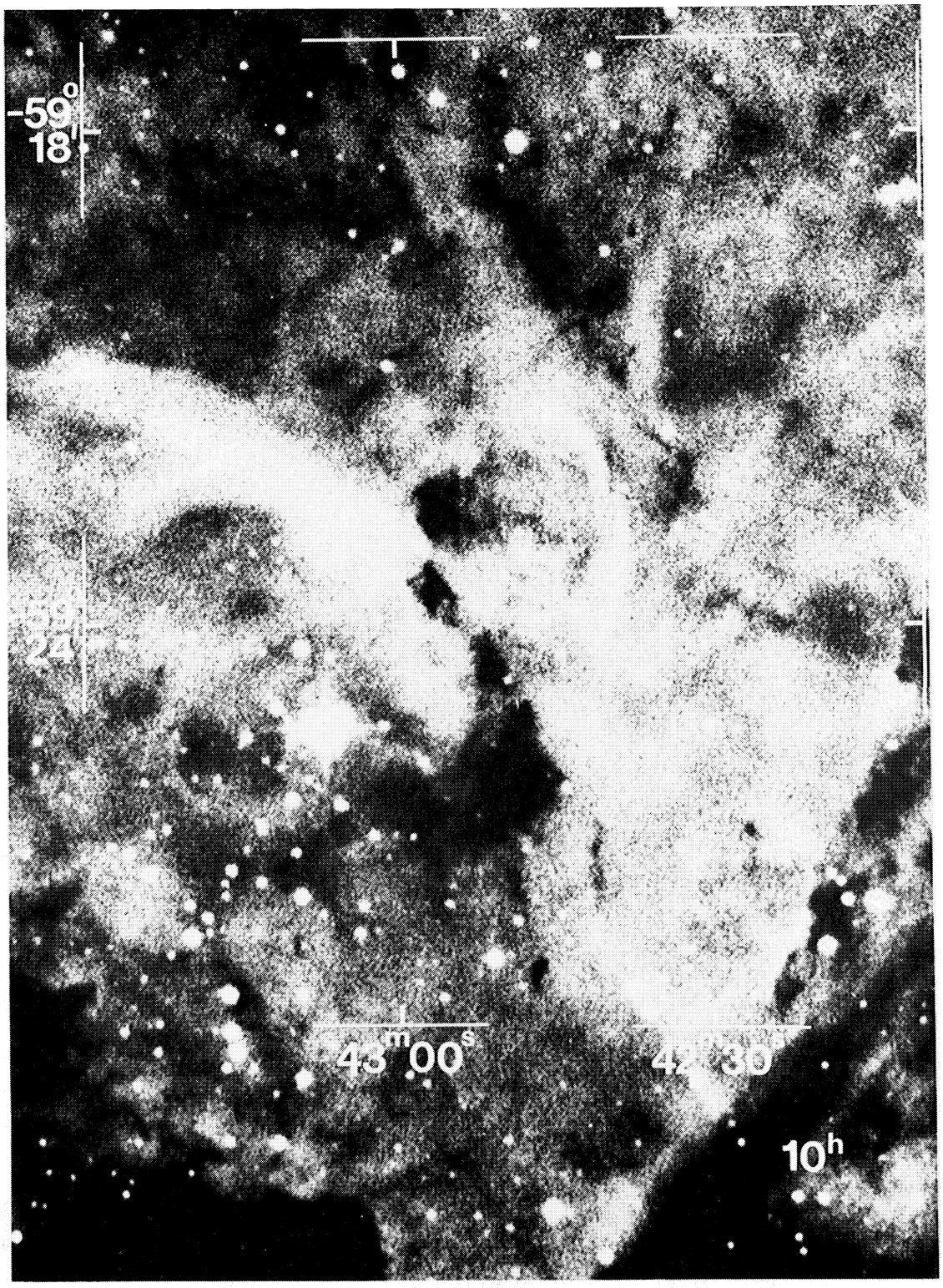

Fig. 2 (Plate 2). As for Fig. 1 (Plate 1) but taken through an interference filter centered on the Hα + [N II] lines. The complex structure of the nebula as well as the conspicuous dark lanes in the region are well revealed in the light of these ions.